Mon. Not. R. Astron. Soc. **352,** 226–232 (2004) doi:10.1111/j.1365-2966.2004.07915.x

A pair of reddened young star clusters in Centaurus

E. Bica,[1] S. Ortolani,[2] Y. Momany,[2] C. M. Dutra[3] and B. Barbuy[4]★

[1]*Universidade Federal do Rio Grande do Sul, Departamento de Astronomia, CP 15051, Porto Alegre 91501-970, Brazil*
[2]*Università di Padova, Dipartimento di Astronomia, Vicolo dell'Osservatorio 5, I-35122 Padova, Italy*
[3]*Universidade Estadual do Rio Grande do Sul, Unidade São Borja, Rua Bompland 512, São Borja 97670-000, RS, Brazil*
[4]*Universidade de São Paulo, Departamento de Astronomia, Rua do Matão 1226, Cid. Universitária, São Paulo 05508-900, Brazil*

Accepted 2004 April 7. Received 2004 March 31; in original form 2003 September 5

ABSTRACT

Photometry in the *BVI* and *JHK* bands is presented for the first time for the southern open clusters Danks 1 and 2, located in the Centaurus region. They are relatively rich and compact, and projected at approximately 4 arcmin from each other. The clusters are very reddened, with $A_V = 8.1 \pm 0.45$ and 9.3 ± 0.6, respectively. They are young clusters, with ages of approximately 10 Myr, and may be related to the 305° H II region complex in the area. Distances from the Sun of $d_\odot \approx 3.6 \pm 0.5$ and 3.4 ± 0.2 kpc are derived for Danks 1 and 2. They might form a physical cluster pair.

Key words: Hertzsprung–Russell (HR) diagram – open clusters and associations: individual: Danks 1 – open clusters and associations: individual: Danks 2.

1 INTRODUCTION

The study of infrared star clusters in the Galaxy is making fast progress, as shown by the detection of the young massive clusters or candidates in the central parts of the Galaxy (Glass, Moneti & Moorwood 1990; Nagata et al. 1990, 1995; Figer, McLean & Morris 1999; Dutra & Bica 2000, 2001), and two obscured globular clusters found in the 2MASS survey (Hurt et al. 2000). Recently a catalogue of infrared (IR) embedded clusters and stellar groups, containing 276 entries, was presented by Bica, Dutra & Barbuy (2003).

Some star clusters are so much reddened that they are close to the limit of optical detectability, like the young open cluster Westerlund 1 (Piatti, Bica & Clariá 1998) and the globular clusters Liller 1 (Frogel, Kuchinkski & Tiede 1995; Ortolani, Bica & Barbuy 1996) and UKS 1 (Minniti, Olszewski & Rieke 1995; Ortolani, Bica & Barbuy 1997). In order to establish the nature and parameters of faint reddened clusters, it is important to compare optical and infrared data, with the aim of better understanding the Galactic structure.

The faint clusters Danks 1 and 2 were reported by Danks et al. (1983, 1984) in an infrared study of the obscured H II region complex at $\ell \approx 305°$ in Centaurus. Danks et al. (1983) also identified a Wolf–Rayet star in the complex, projected close to Danks 2. They derived a visual absorption $A_V \approx 9.2$ and a distance from the Sun $d_\odot \approx 4$ kpc for this star, also known as WR48a. More recently, van der Hucht (2001) estimated $A_V \approx 10.13$ and $d_\odot \approx 1.2$ kpc for WR48a. It is a WC9 star at J2000.0 $\alpha = 13^{\rm h}12^{\rm m}39\overset{\rm s}{.}7$ and $\delta = -62°42'58''$.

Georgelin et al. (1988) studied H II regions in the strip $305° < \ell < 312°$, basically corresponding to the tangent of the Scutum–Crux arm, and the far side of the Sagittarius–Carina arm. Danks 1 and 2, the H II region G305.3+0.1 and WR48a are all projected towards a complex of H II regions known as the 305° complex, which may be a coherent structure located between 3.5 and 4.0 kpc from the Sun.

Danks 1 is also designated as C1310 − 624 and is located at $\ell = 305\overset{\circ}{.}39$, $b = 0\overset{\circ}{.}08$ (J2000.0 $\alpha = 13^{\rm h}12^{\rm m}55^{\rm s}$ and $\delta = -62°40'45''$). Danks 2, or C1309 − 624, is located at $\ell = 305\overset{\circ}{.}33$, $b = 0\overset{\circ}{.}07$ (J2000.0 $\alpha = 13^{\rm h}12^{\rm m}27^{\rm s}$ and $\delta = -62°42'05''$). The clusters are clearly seen in ESO/SERC Schmidt plates, especially in the *R*-band, with angular diameters of approximately 2.1 and 1.2 arcmin, respectively, for Danks 1 and 2. No colour–magnitude diagrams (CMDs) are available for the clusters.

In the present work we study these clusters by means of optical and infrared CMDs and verify their possible connection to the H II region complex and/or the Wolf–Rayet star WR48a. In Section 2, the observations are described. In Section 3, the CMDs of the clusters are discussed and parameters are derived. Concluding remarks are given in Section 4.

2 OBSERVATIONS AND REDUCTIONS

Danks 1 and 2 were observed at ESO (La Silla) with the 1.54-m Danish telescope on 2000 March 5 in the optical and at the 3.5-m New Technology Telescope (NTT) on 2000 July 2 and 2002 July 6 in the IR. The log of observations is given in Table 1.

We used the DAOPHOT II and ALLSTAR (Stetson 1987, 1994) packages for stellar photometry in both optical and IR.

2.1 Optical data

For the *B*, *V* and *I* observations, the Danish Faint Object Spectrograph and Camera (DFOSC) and a Loral/Lesser CCD detector C1W7 with 2052 × 2052 pixels were used. The pixel size is 15 μm, corresponding to 0.39 arcsec on the sky and a full field of 13 × 13 arcmin^2.

★E-mail: barbuy@astro.iag.usp.br

Table 1. Log of observations.

Target	Telescope	Filter	Date	Exp. (sec)	Seeing (arcsec)
Danks 1/2	Danish	V	2000 March 5	60	1.4
		V	2000 March 5	900	1.2
		I	2000 March 5	60	1.2
		I	2000 March 5	600	1.2
		B	2000 March 5	60	1.3
		B	2000 March 5	1800	1.3
	NTT	J	2000 July 2	240	1.1
		H	2000 July 2	240	1.1
		K_S	2000 July 2	240	1.1
		J	2002 July 6	840	0.8
		K_S	2002 July 6	840	0.8

The calibrations have been carried out using Landolt (1983, 1992) standard stars. The derived calibration equations are

$$B = 26.40 + 0.1(B - V) + b, \quad (1)$$

$$V = 26.46 + 0.01(V - I) + v, \quad (2)$$

$$I = 24.61 - 0.01(V - I) + i, \quad (3)$$

reduced to 15 sec (1.15 airmasses) in B, 10 sec in V and 5 sec in I. The zero-point and slope errors of the equations are approximately ± 0.015. The calibration uncertainty is dominated by crowding effects in the determination of the aperture corrections of the cluster stars (± 0.03 mag). The CCD shutter time uncertainty (≈ 0.2 s) related to the short exposures used for the standard stars leads to an additional 2 to 3 per cent error, which is propagated to the calibration of the longer exposure cluster frames. The resulting zero-point uncertainty of our photometry is estimated to be ± 0.05. The atmospheric extinction was corrected using the standard La Silla coefficients ($C_V = 0.13$ and $C_I = 0.1$ mag airmass^{-1}).

2.2 Infrared data

The J and K_S observations at the NTT Nasmyth A port were obtained with the Son of ISAAC (SOFI) camera equipped with the Hawaii 1024 × 1024 HgCdTe detector, with a pixel size of 18.5 μm. Because some cirrus clouds were present in the 2000 observations, we have used additional observations of 2002 July only for calibrations purposes.

The 2000 observations used the SOFI wide-field mode, with scale 0.29 arcsec pixel^{-1} and field 4.9 × 4.9 arcmin^2. A detector integration time (DIT) of 2 s, a number of detector integrations (NDIT) of 30 and a number of exposures (NEXP) of 4 were adopted.

The 2002 observations were obtained with the same instrumentation in small field mode with scale 0.135 arcsec pixel^{-1} and field 2.45 × 2.45 arcmin^2. For the J filter we used DIT of 10 s, an NDIT of 6 and an NEXP of 14, whereas in the K_S filter we used 7 s, 7 and 18, respectively.

Infrared observations require sky subtraction as a result of thermal emission. The subtraction technique was that for small objects or uncrowded fields, according to the SOFI Users Manual (Lidman et al. 2000). The standard stars 9150, 9157 and 9170 from Persson et al. (1998) were observed at different airmasses. For each standard star, five measurements of 2 s for each airmass were obtained.

Dark frame subtraction, sky subtraction and flat fielding were applied. We used illumination correction frames and the bad pixels masks, available from the ESO web pages[1] for flat fielding.

[1] http://www.ls.eso.org/lasilla/sciops/ntt/sofi/reduction/flat_fielding.htm

We used a K_S filter and we consider that this introduces an extra uncertainty in the K filter calibration of ± 0.02 mag (e.g. Ivanov et al. 2000). The instrumental magnitudes of the standard stars were normalized to 1-s exposure and zero airmass, according to the following equation:

$$m' = m_{ap} + 2.5 \log(t_{exp}) - K_\lambda X, \quad (4)$$

where m_{ap} is the mean instrumental magnitude of the five measurements in a circular aperture of radius $R = 5.2$ arcsec, X is the mean airmass and t_{exp} is DIT in seconds. The mean extinction coefficients adopted for La Silla are $K_J = 0.08$ and $K_K = 0.05$ (from ESO web pages). A least-squares fit of the normalized instrumental magnitudes to the magnitudes of Persson et al. (1998) gave the following relations:

$$J - j = 23.07, \quad (5)$$

$$K - k_S = 22.34. \quad (6)$$

Colour terms are negligible. The rms scatter of the residuals of the fit is 0.03 and 0.02 mag in J and K, respectively. Together with transformation from the K_S to K filter, this yields total uncertainties of 0.03 and 0.04 in the J and K bands, respectively.

The photometric extractions were performed on the stacked images using ALLSTAR. The final calibrated magnitudes took into account aperture corrections applied to point spread function (PSF) magnitudes.

2.3 Objects in the field

We show in Fig. 1 a V 15 min exposure frame of an extraction of 6 × 6 arcmin^2 containing Danks 1 and 2. Danks 1 is the larger and looser cluster to the east and Danks 2 is more compact and is located close to the brightest field star. The Wolf–Rayet WR48a is the bright star at ∼1.5 arcmin southeast of Danks 2.

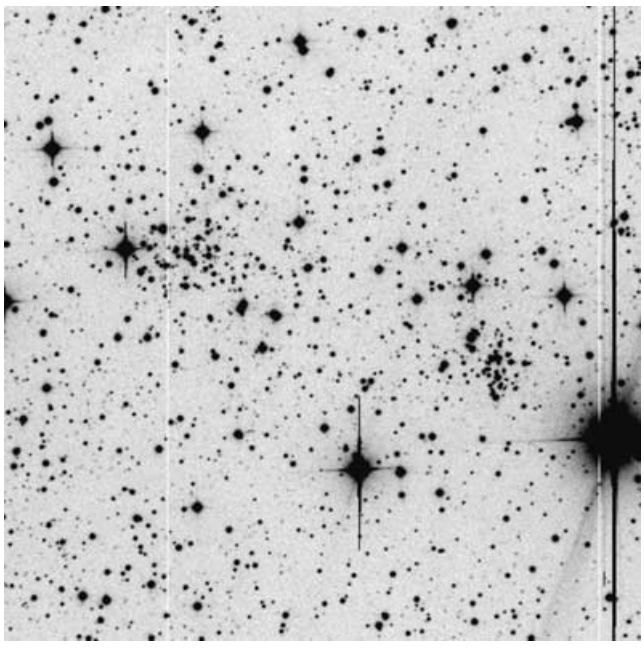

Figure 1. 15-min V image of Danks 1 and 2. Danks 1 is the looser eastern cluster. The Wolf–Rayet WR48a is the rather bright star located 1.5 arcmin south-east of Danks 2. The extraction is 6 × 6 arcmin^2. North is up and west is to the right.

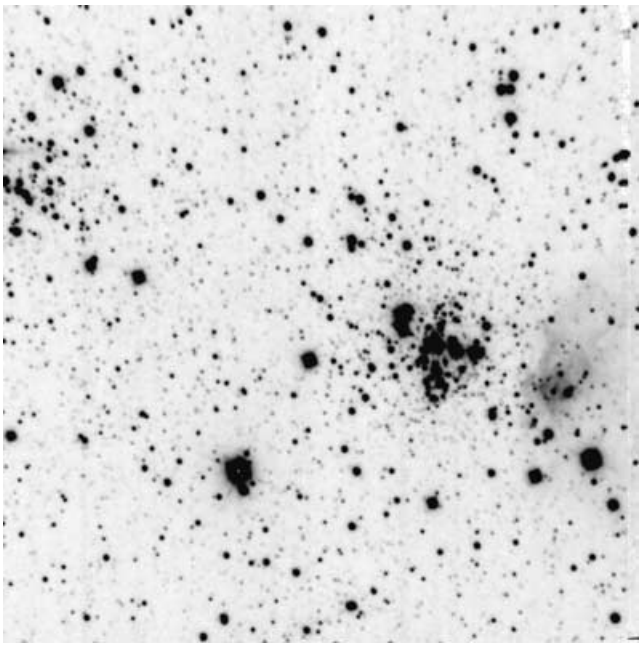

Figure 2. 4 min exposure K_S image of Danks 1 (left, partially included), Danks 2 (right) and the closely projected radio H II region G305.3+0.1 (right edge). North is up and west is to the right. Dimensions are 4.9×4.9 arcmin^2.

In Fig. 2 is presented a 4 min exposure K_S image of Danks 1 and 2 from the 2000 run. In this figure an H II region is projected $\approx$1 arcmin west of the cluster. As can be seen in the image, part of Danks 1 is out of the K_S frame. For the subsequent photometry involving this band, the eastern part of the cluster is therefore not included. This H II region, designated as G305.3+0.1 or G305.32+0.07, is present in the radio survey by Shaver & Goss (1970) and is also identified in Danks et al. (1984). The H II region is absent in the V image (Fig. 1) as a result of a high reddening and in Fig. 2 it has a size of approximately 1.9 arcmin.

3 COLOUR–MAGNITUDE DIAGRAMS

3.1 Optical CMDs

In Fig. 3 is shown the V versus $B - V$ whole field diagram. The dominant (bluest) feature is a disc main sequence (MS). It is considerably widened by differential reddening. The stars on the red side seem to be a mixture of evolved disc stars and a population related to the clusters and probably also to the $l = 305^\circ$ complex. The large colour separation between the two sequences (approximately $\delta(B - V) = 1$) could be produced by the reddening of an intervening dust cloud, HMSTG335.1+0.2 (Hartley et al. 1986).

In Figs 4 and 5 we show V versus $B - V$ extractions of $r <$ 59 arcsec ($r < 150$ pixels) and $r < 78$ arcsec ($r < 150$ pixels) for Danks 1 and 2, respectively. In both cases, the clusters correspond to the redder sequences. The Danks 2 MS is redder than that of Danks 1, as a result of a higher reddening. Differential reddening is important for both clusters.

In Figs 6 and 7 we show V versus $V - I$ with the same extractions of Figs 4 and 5 for Danks 1 and 2. The sequences are better defined than in Figs 4 and 5, as a result of the reduced effects of differential reddening.

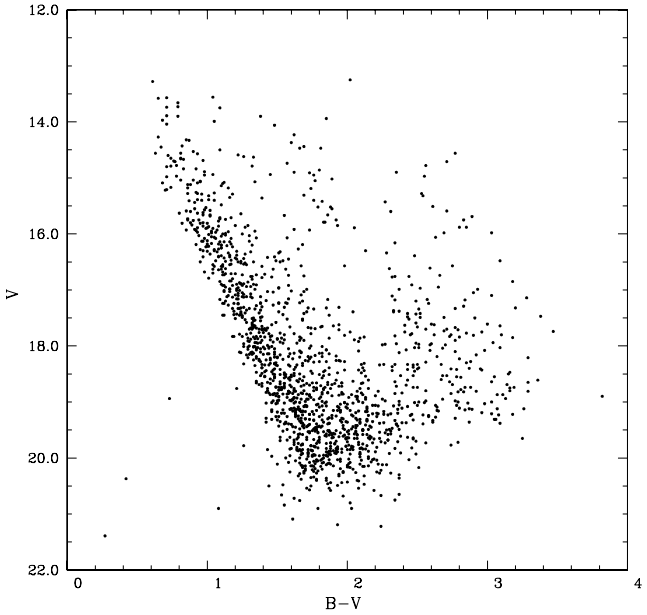

Figure 3. Whole field (13×13 arcmin) V versus $B - V$.

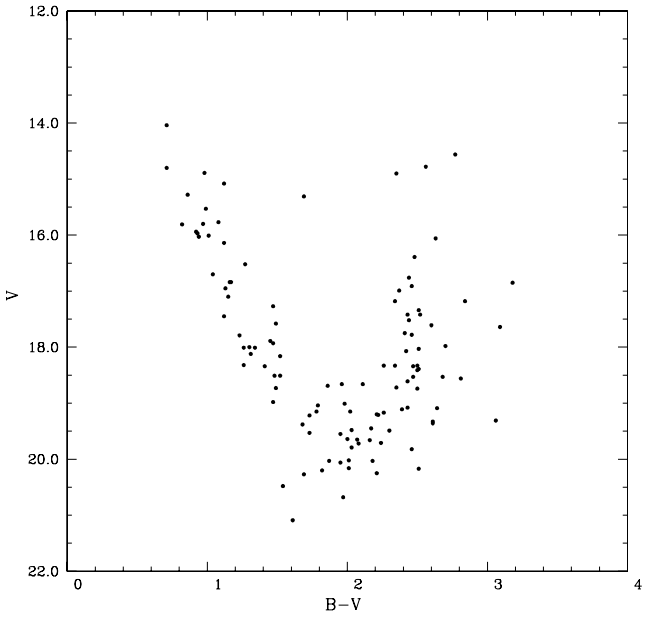

Figure 4. Danks 1: V versus $B - V$ diagram for an extraction of $r <$ 150 pixels ($r < 59$ arcsec). Danks 1 corresponds to the red sequence.

3.2 Infrared CMDs

In Fig. 8 the J versus $J - K$ diagram for the whole field is shown. Compared to Fig. 3, the blue feature (disc MS) is less pronounced whereas the redder features containing the clusters are dominant in the infrared.

In Fig. 9 we show an angular extraction of $r < 110$ pixels ($r <$ 32 arcsec) of Danks 1 in J versus $J - K$ and in Fig. 10 an extraction of $r < 90$ pixels ($r < 26$ arcsec) of Danks 2. Danks 1 shows a better defined MS than Danks 2. The extended MS suggests young ages in both cases. In Fig. 9, for the fainter magnitudes, there is evidence of pre-MS stars, although photometric errors may be important. Note that the extractions for the infrared CMDs are smaller than those

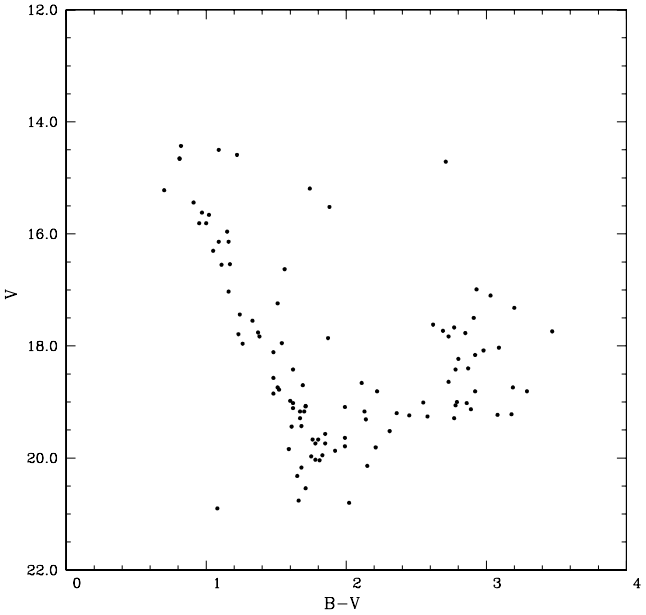

Figure 5. Danks 2: V versus $B - V$ diagram for an extraction of $r <$ 150 pixels ($r < 78$ arcsec). Danks 2 corresponds to the red sequence.

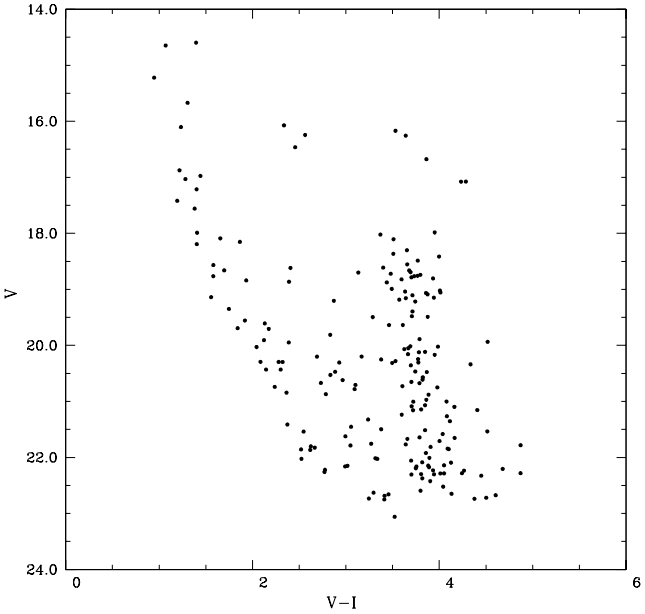

Figure 7. Danks 2: V versus $V - I$ diagram for an extraction of $r <$ 150 pixels ($r < 78$ arcsec).

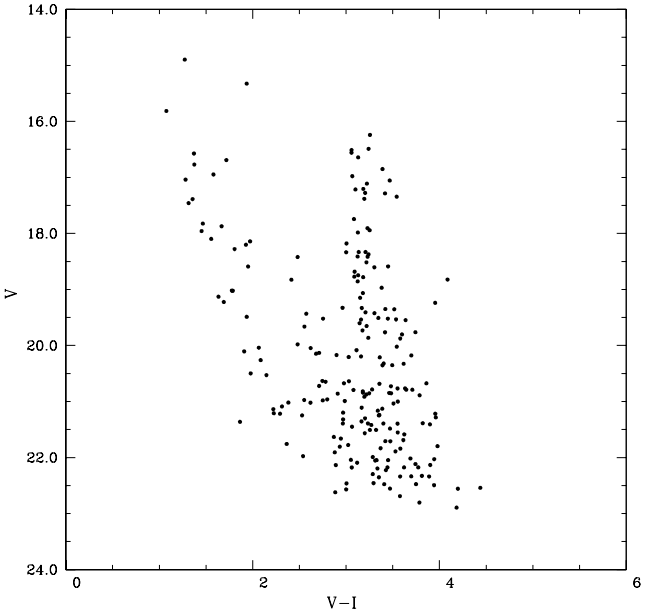

Figure 6. Danks 1: V versus $V - I$ diagram for an extraction of $r <$ 150 pixels ($r < 59$ arcsec).

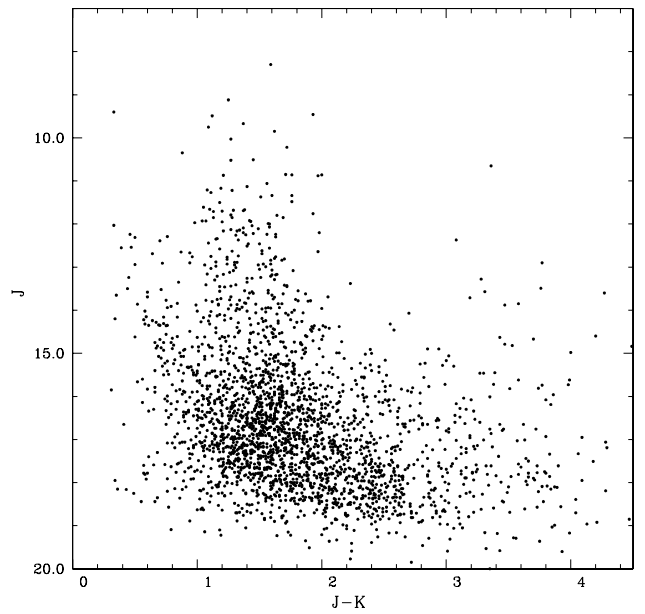

Figure 8. Whole field (4.9×4.9 arcmin^2) J versus $J - K$.

from the optical. This is the result of tests to minimize contamination and differential reddening in these diagrams. In the IR, the less pronounced spread allows to better define the cluster CMD features.

3.3 Cluster parameters

3.3.1 Age

With respect to the optical, the IR CMDs are better defined and are more suitable for age determinations. The shape of the upper MS is an age constraint. We used Padova isochrones of solar metallicity (Bertelli et al. 1994). The resulting best fit for Danks 1 (Fig. 9) is $10\pm^{20}_{5}$ Myr. Isochrones older than 30 Myr clearly do not fit the data. The same age is compatible for Danks 2, but uncertainties are larger.

The bright star at $J = 8.3$ constrains considerably the age of Danks 1. However if it is not a member, or a post-MS star, combinations of ages and distances may produce alternative solutions, because both these parameters cause vertical shifts for such young objects.

3.3.2 Reddening

We derive the reddening from the colour difference between the observations and the theoretical isochrone. An alternative method is

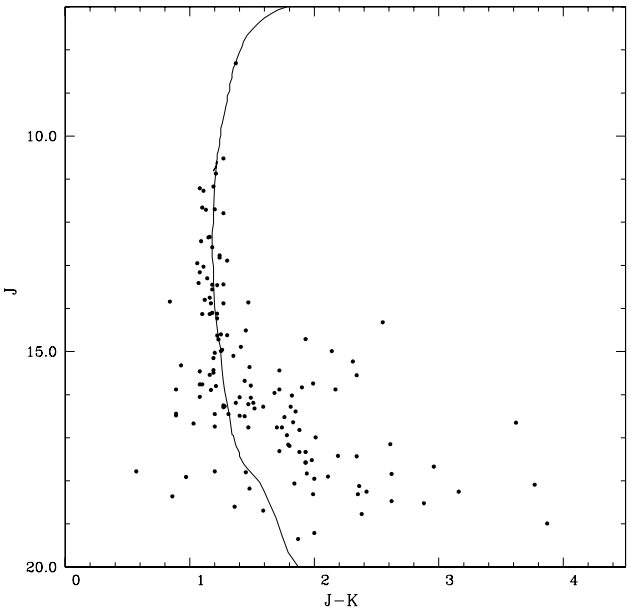

Figure 9. Danks 1: J versus $J - K$ diagram for an extraction of $r <$ 110 pixels ($r < 32$ arcsec). A Padova isochrone of 10 Myr is superimposed.

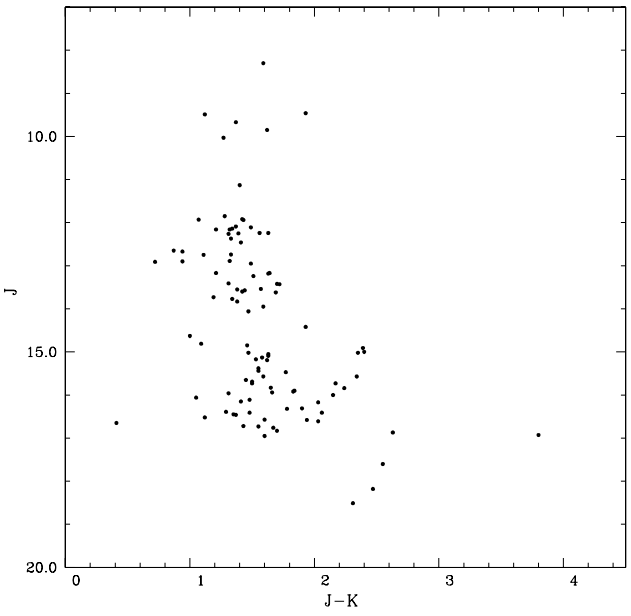

Figure 10. Danks 2: J versus $J - K$ diagram for an extraction of $r <$ 90 pixels ($r < 26$ arcsec).

to compare the observed colours of the upper MS cluster stars with the intrinsic colours of nearby massive MS stars as compiled by Binney & Merrifield (1998, and references therein). From Fig. 4(a) we derive a value of $E(B-V) = 2.6 \pm 0.15$ for Danks 1 and $E(B-V) = 3.0 \pm 0.2$ for Danks 2. Errors are estimated from the width of the MS. This gives absorptions of $A_V = 8.1 \pm 0.45$ and 9.3 ± 0.6, respectively.

We apply the same procedures for the infrared colours and use $E(J-K) = 0.51E(B-V)$, from the absorption values of Schlegel, Finkbeiner & Davis (1998). We get $E(J-K) = 1.35 \pm 0.1$, converting to $E(B-V) = 2.65 \pm 0.2$ for Danks 1 and $E(J-K) = 1.50 \pm 0.2$, giving $E(B-V) = 2.95 \pm 0.4$ for Danks 2. There is an excellent agreement with the optical results.

3.3.3 Distance

We applied a method of probable similarity of an nth star in young open clusters of comparable ages, to have a given luminosity in the MS. A similar method was used by Dutra & Bica (2001) in a study of embedded clusters in Cygnus X, where they adopted the 10th brightest star for distance estimates. The method is a useful tool in cases of young clusters for which no spectral type information is available. In the present paper, after a few checks on different young clusters, we found it appropriate to take the 10th brightest star in the blue CMD sequence, to ensure a comparable MS level. As comparison clusters we use the composite CMDs of ages 5, 10, 15 and 22 Myr (cluster groups of NGC 6231, 884, 457 and 3755) from Mermilliod (1981a,b). We obtained for the 10th brightest star $M_V = -4.6 \pm 0.7$. According to Binney & Merrifield (1998), this absolute magnitude corresponds to a B0/O8 star MS star. We assume that it is a B0 star, with $M_V = -4$. For Danks 1 and 2, the 10th brightest stars have $V = 16.6 \pm 0.6$ and $V = 17.86 \pm 0.5$, respectively. These values are from both the BV and VI CMDs. These values, combined with the absorptions derived in Section 3.3.2, yield $(m-M)_0 =$ 12.2 and 11.9, and distances to the Sun $d_\odot = 2.8$ and 2.4 kpc, respectively. The uncertainties may amount to 1 kpc. The main source of uncertainty in this method is the assumption of the spectral type of the 10th brightest star. In the present case, given that the clusters show no gas emission, O-type stars can be ruled out.

From similar calculations for the IR (Figs 9 and 10), we get as 10th brightest star $J = 11.7$ and 12.0 for Danks 1 and 2. Adopting $A_J = 0.276\, A_V$ (Schlegel et al. 1998), we get $A_J = 2.24$ and 2.57. For a B0 star $M_J = -3.32$ and the distance moduli are $(m-M)_0 =$ 12.78 and 12.75. The resulting distances are $d_\odot = 3.6$ and 3.5 kpc, respectively.

Finally, we can use isochrones on the better defined sequence of Danks 1, as shown in Fig. 9. The fit provides $(m-M)_J = 15.3$, which leads to $d_\odot = 4.1$ kpc.

Averaging the different determinations we get $d_\odot = 3.6 \pm 0.5$ and 3.4 ± 0.2 kpc for Danks 1 and 2. The errors correspond to the deviations from the average.

In order to constrain the above distances better, spectroscopy of the brightest MS stars is required to obtain their spectral types.

We assume the distance of the Sun to the Galaxy centre to be $R_\odot = 8.0$ kpc (Reid 1993). The Galactocentric coordinates for Danks 1 are $X = -5.5$ kpc ($X < 0$ refers to our side of the Galaxy), $Y = -3.0$ kpc and $Z = 0.01$ kpc. The distance from the Galactic centre is $R_{\rm GC} = 6.3$ kpc and the distance projected on the plane $r_{\rm GC}$ is approximately the same. Danks 2 is at a similar position as Danks 1 within errors and they might form a physical cluster pair.

Concerning the Wolf–Rayet star WR48a, the recent distance determination of 1.2 kpc by van der Hucht (2001) is much closer than the previous value by Danks et al. (1983) of 4 kpc, which in turn is compatible with the present determinations for the Danks clusters. In the first case, the star and the clusters are not related.

3.4 The radio H II region G305.3+0.1

In Figs 11 and 12 we compare an extraction of radius $r < 80$ pixels ($r <$ 23 arcsec) of the radio H II region G305.3+0.1 with an adjacent field of equal area. In Fig. 11 there is an excess of bright stars ($J > 15$) and $J - K \approx 1.8$, suggesting them to be the upper MS

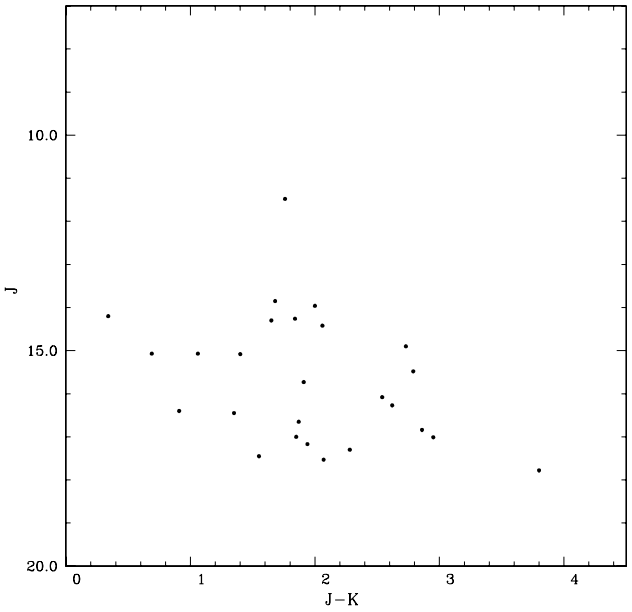

Figure 11. H II region G305.3+0.1: J versus $J - K$ diagram for an extraction of $r < 80$ pixels ($r < 23$ arcsec).

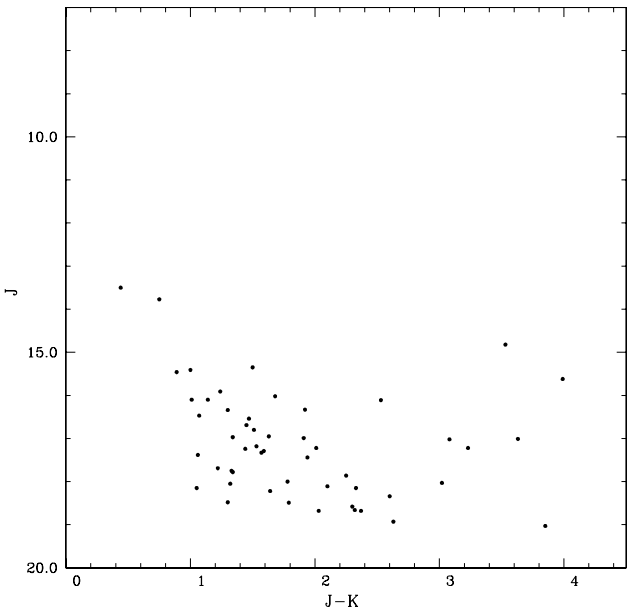

Figure 12. Same as Fig. 11 for the offset field.

stars of the H II region, responsible for the ionization. Their colour is compared to O3/B0 stars of intrinsic colour $J - K = -0.05$ (Binney & Merrifield 1998) and we obtain $E(J - K) = 1.80$, converting to $E(B - V) = 3.63$, and $A_V = 11.25$ ($A_J = 3.11$). Assuming that the brightest star at $J = 11.5$ is an O3 type ($M_J = -5.27$), then the distance from the Sun would be $d_\odot = 5.4$ kpc. The clump of stars at $J = 14.15$, therefore basically correspond to B0-type stars of $M_J \approx -3.32$ and we derive a distance of $d_\odot = 7.4 \pm 1.2$ kpc. Alternatively, if we assume as an extreme case that the brightest star could be a B0 star, the distance would be only 2.2 kpc. We argue that a shorter distance or an intermediate situation, with a distance comparable with that of Danks 2 is more likely, because Danks 2 has a higher differential as well as absolute reddening as compared with Danks 1. Dust from the H II region could be responsible for this extra reddening.

4 CONCLUSIONS

We conclude that the open clusters Danks 1 and 2 are young ($\approx$10 Myr) and strongly reddened ($A_V = 8.1 \pm 0.45$ and 9.3 ± 0.6, respectively). The derived distances of $d_\odot = 3.6 \pm 0.5$ and 3.4 ± 0.2 kpc place them at a compatible distance with the $\ell = 305^\circ$ complex. The closely projected radio H II region G305.3+0.1 might be spatially close to Danks 2 and responsible for the higher absolute and differential reddening affecting Danks 2 as compared with Danks 1.

The location of the clusters in the Galaxy appears to be in the Scutum–Crux arm (Georgelin et al. 1988; Taylor & Cordes 1993). An important source of absorption for the clusters may arise from the dust cloud HMSTG335.1+0.2 (Hartley et al. 1986), which is supposed to be located in the foreground (Sagittarius–Carina arm).

These two clusters have a projected separation of approximately 4 arcmin, which converts into 4 pc at a common distance of $\sim$3.5 kpc. They could form a physical pair, a rare case among open clusters but not among very young embedded infrared star clusters, for which the fraction of pairs and triplets is as high as 25 per cent (Bica et al. 2003).

ACKNOWLEDGMENTS

The authors acknowledge partial financial support from CNPq and Fapesp. SO acknowledges Italian Ministero dell'Università e della Ricerca Scientifica e Tecnologica (MURST) under the programme on 'Stellar Dynamics and Stellar Evolution in Globular Clusters: a Challenge for New Astronomical Instruments'.

REFERENCES

Bertelli G., Bressan A., Chiosi C., Fagotto F., Nasi E., 1994, A&AS, 106, 275
Bica E., Dutra C., Barbuy B., 2003, A&A, 397, 177
Binney J., Merrifield M., 1998, in Ostriker J.P., Spergel D.N., eds, Galactic Astronomy. Princeton Univ. Press, Princeton, NJ, p. 107
Danks A.C., Dennefeld M., Wamsteker W., Shaver P.A., 1983, A&A, 118, 301
Danks A.C., Wamsteker W., Shaver P.A., Retallack D.S., 1984, A&A, 132, 301
Dutra C.M., Bica E., 2000, A&A, 359, L9
Dutra C.M., Bica E., 2001, A&A, 376, 434
Figer D.F., McLean I.S., Morris M., 1999, ApJ, 514, 202
Frogel J.A., Kuchinkski L.E., Tiede G.P., 1995, AJ, 109, 1154
Georgelin Y.-M., Boulestex J., Georgelin Y.-P., Le Coarer E., Marcelin M., 1988, A&A, 205, 95
Glass I.S., Moneti A., Moorwood A.F.M., 1990, MNRAS, 242, 55
Hartley M., Manchester R.N., Smith R.M., Tritton S.B., Goss W.M., 1986, A&AS, 63, 27
Hurt R.L., Jarret T.H., Kirkpatrick J.D., Cutri R.M., Schneider S.E., Skrutskie M., van Driel W., 2000, AJ, 120, 1876
Ivanov V.D., Borissova J., Alonso–Herrero A., Russeva T., 2000, AJ, 119, 2274
Landolt A.U., 1983, AJ, 88, 439
Landolt A.U., 1992, AJ, 104, 340
Lidman C., Cuby J.G., Vanzi L., 2000, in SOFI users manual Doc. No. LSO-MAN-40100-003, issue 13
Mermilliod J.C., 1981a, A&AS, 44, 467
Mermilliod J.C., 1981b, A&A, 97, 235
Minniti D., Olszewski E., Rieke M., 1995, AJ, 110, 1686

Nagata T., Woodward C.E., Shure M., Pipher J.L., Okuda H., 1990, ApJ, 351, 83
Nagata T., Woodward C.E., Shure M., Kobayashi N., 1995, AJ, 109, 1676
Ortolani S., Bica E., Barbuy B., 1996, A&A, 306, 134
Ortolani S., Bica E., Barbuy B., 1997, A&AS, 126, 319
Persson S.E., Murphy D.C., Krzeminski W., Roth M., Rieke M.J., 1998, AJ, 116, 247
Piatti A.E., Bica E., Clariá J.J., 1998, A&AS, 127, 423
Reid M., 1993, ARA&A, 31, 345
Schlegel D.J., Finkbeiner D.P., Davis M., 1998, ApJ, 509, 525
Shaver P.A., Goss W.M., 1970, Aust. J. Phys. Astrophys., 14, 77
Stetson P.B., 1987, PASP, 99, 191
Stetson P.B., 1994, PASP, 106, 250
Taylor J.H., Cordes J.M., 1993, ApJ, 411, 674
van der Hucht K.A., 2001, New Astron. Rev., 45, 135

This paper has been typeset from a TEX/LATEX file prepared by the author.